FluChe: Fluorescence and Cherenkov light detection with SiPM for space and ground applications

O. Catalano[1], G. Contino[1], G. Sottile[1], P. Sangiorgi[1], M. Capalbi[1], D. Mollica[1], G. Osteria[2], V. Scotti[2,3], H. Miyamoto[4,5], C. Vigorito[4,5], M. Casolino[6,7], C. De Donato[7], S. Ahmad[8], J.B. Cizel[8], J. Fleury[8], M. Morenas[8], F. Perez[8]

[1] Istituto Nazionale di Astrofisica - Istituto di Astrofisica Spaziale e Fisica Cosmica di Palermo, Via Ugo la Malfa 153, 90146 Palermo, Italy, e-mail: `osvaldo.catalano@inaf.it`
[2] Istituto Nazionale di Fisica Nucleare - Sezione di Napoli, Strada Comunale Cinthia, 80126 Napoli, Italy
[3] Università degli Studi di Napoli Federico II - Dipartimento di Scienze Fisiche, Via Cinthia, 80126 Fuorigrotta Napoli, Italy
[4] Istituto Nazionale di Fisica Nucleare - Sezione di Torino, Via Pietro Giuria 1, 10125 Torino, Italy
The remaining affiliations can be found at the end of the paper.

Abstract. Space and ground missions measuring extensive air showers produced by cosmic rays, gamma rays and neutrinos in atmosphere require detection of very faint and intense ultraviolet-visible light with different time scale. The characteristics of the new generation of Silicon PhotoMultiplier (SiPM) are suitable for this purpose, especially for space missions that require: robustness against exposure to light, low weight, low power consumption and high intrinsic gain. The high-performance detection power of SiPMs makes them promising for charge integration, where the total amount of charge in the signal is required, as well as for photon counting, where extreme photodetector sensitivity is needed, as in case of Cherenkov and fluorescence light detection. The capability to operate SiPM contemporarily in both modes is strictly dependent indeed by the design of the Front-End Electronics (FEE). The most important challenge is to find the right balance and a feasible solution for managing SiPM with a FEE to be able to work, contemporarily and efficiently, in photon counting and charge integration. In this paper we present RADIOROC, a new ASIC that will be able to work contemporarily in both modes: in this way it will be capable to acquire both Cherenkov and fluorescence signals. RADIOROC is going to be used in the innovative experiment MUCH, a telescope that uses the Imaging Atmospheric Cherenkov technique to detect Cherenkov light from muons for volcanoes radiography (muography) and wherever it is required a non-invasive radiographic inspection of geological or engineering structures, even of considerable size.

Key words. Cosmic Rays – Gamma Rays – Neutrinos – SiPM – ASIC – Cherenkov – Fluorescence – Muography

1. Introduction

In the last decades several researches and experiments have been devoted to the detection and study of the energetic particles coming from the outer space, first of all Cosmic Rays and Gamma Rays. For what concerns experiments requiring light detection, some of them need detection of very intense light, some of very faint light and some other in between with different time scale and time resolution. Covering the entire range of observable ultraviolet-visible (UV-VIS) wavelengths requires the design of a specific photo-detector module that shall embed a dedicated Front-End Electronics (FEE) which uses the two modalities, photon counting and charge integration, concurrently within a single read-out front-end ASIC (Application-Specific Integrated Circuit). This allows an unprecedented measurement precision from the single photon to the maximum of the photo-detector dynamic range. For maximum usability and flexibility, single-photon-counting as well as charge integration should coexist and be activable by the user on the same front-end ASIC. In this paper we present the design of a novel ASIC which will be able to manage most of the detectors of those instruments that require light detection in the UV-VIS wavelength band. The objectives of this new chip and the experimental application fields in which it could be potentially used are briefly discussed. Together with the description of the new ASIC, named RADIOROC (RADIOgraphy Read Out Chip), and its innovative features, we report on the measurement results performed in the laboratory.

2. Objectives of the new ASIC

Among the several application fields, RADIOROC aims to fulfil the requirements of many high energy physics projects devoted to the detection of Cherenkov and fluorescence light produced by particles from space and at ground.

The Cherenkov light is emitted by secondary charged particles, generated in the interaction of primary particles with the Earth's atmosphere (Watson , 2011). The Cherenkov light production occurs when a charged particle (like an electron) passes through a dielectric medium, the air in our case, at a speed faster than that of light in that medium. The charged particles polarize the air molecules, which then quickly return to their fundamental state, emitting photons in the direction of travel of the charged particles producing a very short (a few ns) and feeble (a few tens of photons per meter) light emission in the UV-VIS wavelengths.

The fluorescence light is emitted by the same type of secondary charged particles (Keilhauer et al. , 2013). Their energy deposit in air by ionization and excitation of air molecules causes fluorescence light emission in a large number of spectral lines which are very close to each other. The strongest emissions occur in the wavelength region between 300 and 400 nm with a resulting fluorescence yield of about 4 photons per meter.

Cherenkov and fluorescence light can only be detected during the night by means of telescopes with large optical collecting surfaces and with fast and very sensitive multi-pixel cameras.

While Cherenkov light is emitted in a very short time in a beamed cone, fluorescence light is emitted isotropically with a long time track progression (tens of microseconds). The wide differences between the two phenomena should mean that one detection method excludes the other. RADIOROC, with its wide detection applicability in the UV-VIS wavelength range, as shown in Fig. 1, is capable to manage the light detectors contemporarily and efficiently using single photon counting and charge integration, making it possible to use the same FEE for different phenomena and potentially for different experiments.
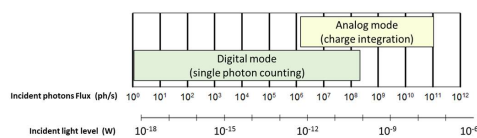

Fig. 1. RADIOROC Digital and Analog mode detection applicability range.

3. RADIOROC application fields

The characteristics of RADIOROC make it eligible for most of the experiments devoted to the detection of fluorescence and Cherenkov light as in Cosmic Rays, Gamma Rays and muons detection.

3.1. Cosmic Rays

Cosmic rays are high-energy radiation which originate from the outer space and move at nearly the speed of light. Some of them reach the Earth and, upon impact with the atmosphere, produce cascades of secondary particles that reach the surface: these cascades are called Extensive Air Showers (EASs). Particles belonging to EASs produce also Cherenkov and fluorescence light as mentioned in section 2. One of the key features of cosmic rays is their energy spectrum which covers 14 orders of magnitude in energy and 32 orders of magnitude in flux: this leads to a very low flux at higher energies, so the most energetic ones are the least known. For the cosmic rays which have an energy greater than 10^{20} eV, the flux of events is very low ($\sim$ 1 $particle$ / 100 km^2 / $year$) and so the only way to have a reasonable statistics is to have a very large collecting area; for this reason, after the biggest existing cosmic rays' observatory (Auger Observatory with its 3000 km^2, Dova et al. , 2003 [1]) the next step is to look downward at the dark earth atmosphere from an observatory placed in orbit. The two big projects devoted to this goal will be EUSO (Extreme Universe Space Observatory, Takahashi et al. , 2009 [2]) and POEMMA (Probe of Extreme Multi-Messenger Astrophysics, Olinto et al. , 2017), that will especially look for Ultra High Energy Cosmic Rays (UHECRs), which have an energy greater than 10^{18} eV. These projects aim to detect also rare events like tau neutrinos and cosmogenic neutrinos.

3.2. Gamma Rays

High-energy gamma rays are photons with energies higher than few tens of GeVs (1 Gev = 10^9 eV). High-energy gamma rays traveling in a straight line from their source to an observer may reveal the astronomical source of cosmic rays. For energies above a few hundred GeVs, a direct measurement of the primary gamma rays from space with stratospheric balloons and satellites is impossible (see e.g. Catalano , 2018): the flux of these quanta is greatly reduced as the energy increases, so the space limitation of the detection surface, necessary to intercept them, makes the observation inefficient. We then rely on an indirect measurement, the detection of secondary particles produced by the interaction of primary gamma rays with the Earth's atmosphere. For energies up to several hundred TeVs, it is possible to use ground-based telescopes such as Cherenkov telescopes, which are designed for the detection of very-high-energy gamma rays. The next years will be led by the CTA (Cherenkov Telescope Array Acharya et al. , 2017 [3]) observatory, that will consist of different types of telescopes to investigate the gamma universe from 20 GeV to 300 TeV. INAF (Istituto Nazionale di AstroFisica) contributed from the beginning to this project, with the ASTRI-Horn prototype telescope (Pareschi et al. , 2013), which has achieved important results, from its optical validation in November 2016, to the first light in May 2017 and the detection of the Crab Nebula at TeV energies in December 2018 (Lombardi et al. , 2020). After a maintenance and upgrade period, the ASTRI-Horn telescope is now fully operative and ready to resume observations. ASTRI-Horn telescope is the starting point for the ASTRI mini-array international project led by INAF (Antonelli et al. , 2021), which will be the first array, composed of nine ASTRI-like Cherenkov telescopes under construction at Teide Observatory, aiming to observe the most energetic gamma rays at energies above 100 TeV.

---

[1] web link: https://www.auger.org/
[2] web link: https://www.jemeuso.org/

[3] web link: https://www.cta-observatory.org/

3.3. Muography

The ASTRI-Horn experience gives rise to an innovative project, funded by INAF: MUCH (MUography by CHerenkov telescope). It will consist of a Cherenkov telescope performing radiography of volcanoes and of massive structures, using Cherenkov light produced by muons in atmosphere (Catalano et al. , 2016).

The possibility of obtaining high-resolution muon-radiography with a high Signal to Noise Ratio (SNR), capable of providing detailed information on the internal structure of a volcano, offers important perspectives because it allows constraining the forecasting models of the volcanic activity state and, consequently, improves the ability to mitigate the risk associated with paroxysmal events. Through the information on the internal structure of the volcano, alterated zones can also be recognized where potentially dangerous instability phenomena may occur, generated by eruptive events. The most commonly used imaging techniques do not allow to obtain an adequate spatial resolution as they need very long detection time and require the execution of measurement campaigns near the structures of active volcanoes, exposing the involved personnel to a risk. Muon imaging via Cherenkov technique represents a promising alternative compared to common scintillation hodoscopes and will allow an important advancement of the muon-radiography methodology. It will be possible to drastically improve the relationship between signal and noise, to obtain high spatial resolution radiographs of active volcanic structures, even farther from them, and with shorter observation campaigns.

4. RADIOROC characteristics

The characteristics of the new generation of SiPMs are suitable for the missions and researches discussed in the previous sections. Their high intrinsic gain, low power consumption, low weight and robustness against accidental exposure to light are particularly important for spaceborn and ground multipixels imaging cameras. The high-performance detection power of SiPMs makes them promising for photon counting, where extreme photodetector sensitivity is needed, as well as for charge integration, where the total amount of charge in the signal is required. However, the capability to operate SiPM contemporarily in photon counting and in charge integration (to detect both fluorescence and Cherenkov light) is dependent by the design of the FEE. RADIOROC has been designed to achieve such performance: it is an improvement of an existing ASIC, named CITIROC (Cherenkov Imaging Telescope Integrated Read Out Chip), properly designed for the camera of the ASTRI-Horn telescope. The CITIROC characteristics are detailed in the datasheet[4], while for a more detailed explanation regarding CITIROC and the RADIOROC requirements, subsequently implemented by the Weeroc company, refer to Contino et al. (2020).

Despite the great results obtained in the ASTRI-Horn system, CITIROC is not suitable for the detection of fluorescence light, where single photon counting with a double pulse resolution of few ns is needed. RADIOROC fulfils this requirement by improving to over 100 MHz the single photon counting rate at trigger output and other features that we will briefly describe.

RADIOROC is a 64-channel front-end ASIC designed to read out SiPM. It has been desiged by the Weeroc microelectronics company using TSMC (Taiwan Semiconductor Manufacturing Company) 130 nm CMOS technology. In the RADIOROC, single-photon counting and charge integration coexist autonomously. These operational modes are activable by the user by means of a set of programmable functions, implemented through a string of configuration bits, which instruct the front-end on the desired operating mode.

To avoid pulses pile-up, single-photon-counting mode with a double pulse resolution of a few ns ($\approx 5\ ns$) is needed. For this reason, in RADIOROC a programmable pole zero

---

[4] web link: https://www.weeroc.com/my-weeroc/download-center/citiroc-1a/16-citiroc1a-datasheet-v2-5/file
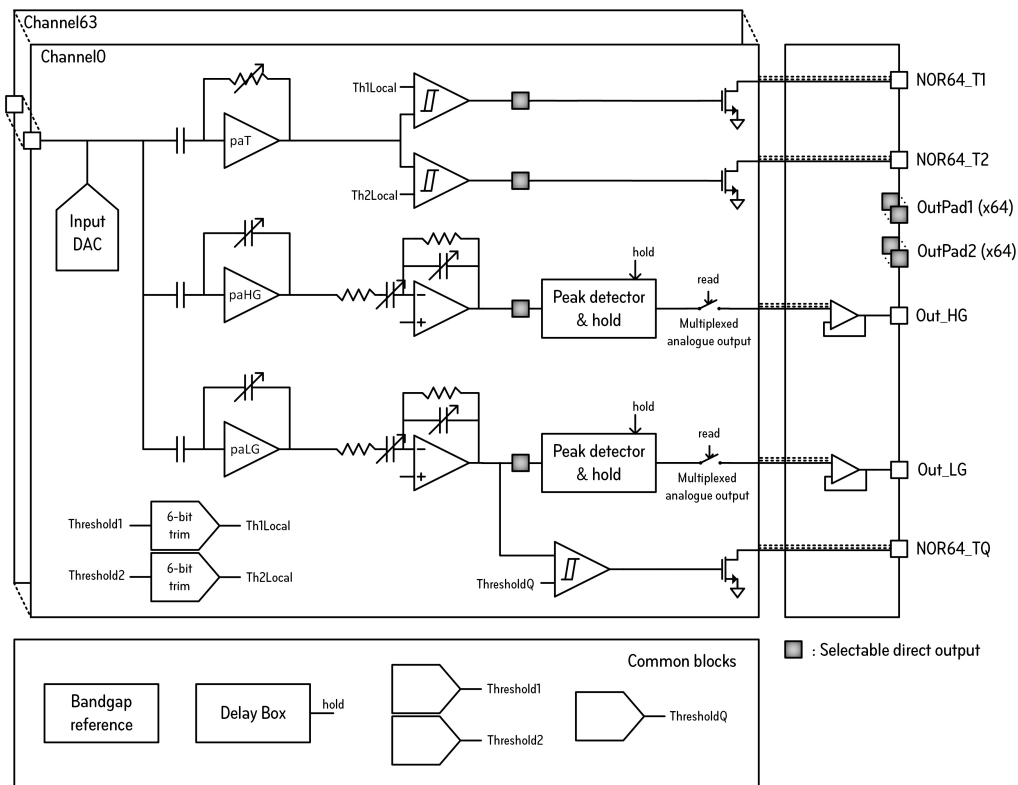
Fig. 2. General block scheme of RADIOROC.

Fig. 3. Picture of the RADIOROC, used for the measurement, mounted on an evaluation board provided by Weeroc.

cancellation circuit that ensures a stable single photon counting up to 200 *MHz* is implemented.

Analog chains based on pulse height measurement technique using peak detector are implemented including pulse-shaping time and pre-amplifier gain programmability in order to cover the desired energy dynamic range. Digital triggers are managed and selectable. Fast discriminators with user adjustable threshold by means of DAC (Digital Analog Converter) provide the digital trigger signals that are routed to a majority/topological trigger logic implemented in the FPGA (Field Programmable Gate Array) connected to the RADIOROC for its operational management. Masking of the digital triggers allows to switch off potential noisy pixels. An adjustment of the SiPM bias voltage is performed using channel-by-channel DAC implemented into the ASIC. This allows for a fine SiPM gain adjustment at the system level to correct for the gain non-uniformity of SiPMs.

The preamplifier used for the trigger is a programmable active high-pass filter with the cut-off frequency chosen to optimize the recovery time of the SiPM. Preamplifiers for charge measurement have been added for SNR and gain optimization. The gain setting is done on the preamplifier and a shaping time setting is done on the shaper circuit. Gain and shaping time setting are for both low and high gain charge measurement. The High Gain charge preamplifier schematic is similar to the trigger preamplifier but with a narrower bandwidth to lower power consumption. It is followed by a shaper circuit for noise filtering and SNR optimization. As for the trigger preamplifier, it is possible a setting on the gain. The preamplifier is followed by a differential shaper circuit. The Low Gain charge measurement is done as the high gain with the input capacitor of the preamplifier being 10 times smaller to have a factor 10 on the gain of the measurement chain. Thanks to these characteristics, high gain and low gain charge measurements have a high precision single photon measurement (with SNR > 10) and a high energy dynamic range, from 1 photo-electron (pe) up to 2000 pe within 1% linearity.

A general block scheme of RADIOROC is shown in Fig. 2 and a picture of the new chip is shown in Fig. 3.

The main characteristics are listed in Fig. 4, while the data sheet of the RADIOROC can be found soon at the Weeroc site[5].

5. RADIOROC measurements

Hereafter we present some measurements carried out on RADIOROC mounted on an evaluation board. These measurements provide basic information about the functionalities of the ASIC which is important in determining the performance characteristics of the design.

RADIOROC	
Detector Read-Out	SiPM,SiPM array
Number of channels	64
Signal Polarity	Positive
Sensitivity	1/3 of photo-electron
Timing Resolution	55 ps FWHM on single photo-electron @ 10^6 SiPM gain
Photon counting	200 MHz
Dynamic range	Up to 2000 photo-electrons @ 10^6 SiPM gain
Packaging & Dimension	BGA 20x20 mm^2
Power Consumption	310 mW – Supply voltage: 1.2 V
Inputs	64 analogue inputs with independent SiPM HV adjustments
Outputs	2 direct outputs per channel, selectable channel per channel, either: - 1 LVDS trigger - 2 TTL triggers - 1 TTL trigger and 1 analog output - 2 analog outputs 2 multiplexed analogue outputs 3 NOR64 trigger outputs
Internal Programmable Features (I^{2}C)	- 64 HV adjustments for SiPM (64 x 8 bits), 3 trigger thresholds tuning - (10 bits), channel by channel gain and shaping time adjustment (τ from 20 ns to 300 ns), individual trigger masking and cell powering

Fig. 4. Main RADIOROC functional characteristics.

5.1. Input DAC

Input DACs are embedded in the RADIOROC ASIC. They are used to adjust the SiPM bias voltage channel-by-channel. Input DACs have 8 bit resolution with an excursion of 550 mV. The input DAC, as shown in Fig. 5, exhibits a good linearity. Differential Non-Linearity (DNL) and Integral Non-Linearity (INL) are shown in Fig. 6.

DAC-inputs are able to sink high DC current (up to 1 mA per channel).

5.2. Threshold DAC

10-bit threshold DACs are used to adjust the discriminator threshold values. There are two threshold DACs, one per discriminator. The two threshold DACs are the same and thus share the same performance. Linearity plot is shown in Fig. 7. DNL and INL are shown in Fig. 8. The worst case error is less than 100 μV.

_____

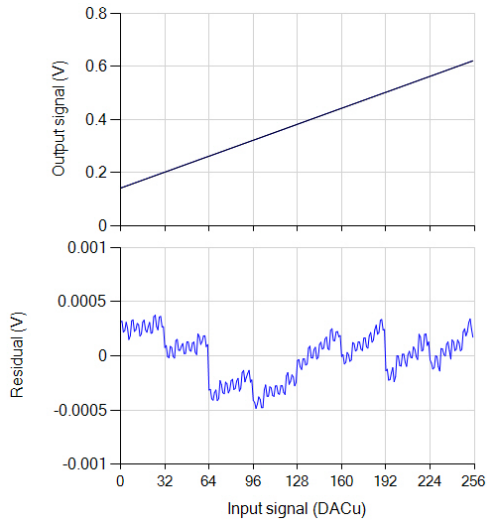[5] web link: https://www.weeroc.com

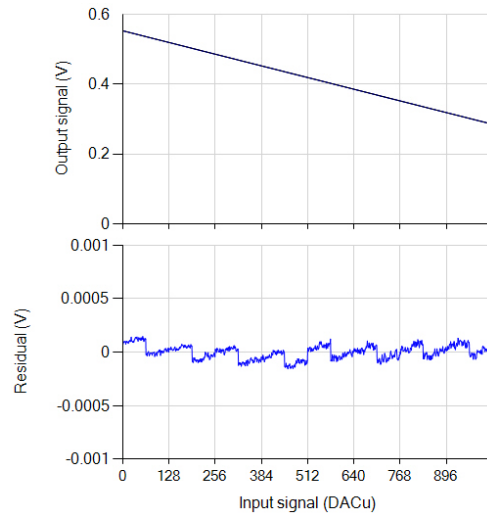**Fig. 5.** Input DAC linearity and residuals.

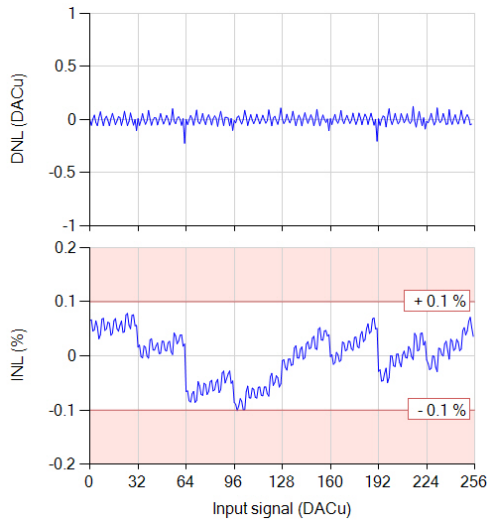**Fig. 7.** 10 bits threshold DACs linearity and residuals.

Fig. 6. INL is better than 0.1% and DNL is better than 0.2 LSB (Least Significant Bit), with a LSB of 2 mV.
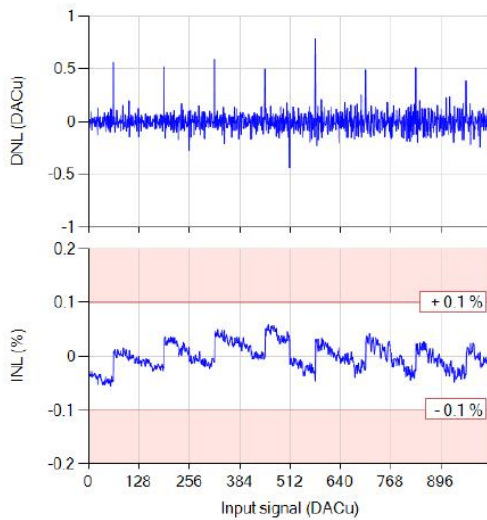

Fig. 8. 10 bits threshold DACs integral and differential non-linearity. INL is 0.1% and DNL is 0.8 LSB.

5.3. Staircase

Staircase plot, shown in Fig. 9, represents the integral distribution of the trigger frequency (*dark count/s*) as DAC threshold increases with the SiPM in dark condition. Staircase is useful to locate the channel pedestal as well as the positions of the first photo-electron and gain in DAC units.

5.4. Charge measurement

Signal pulses height has been measured through the analog shaper output. Fig. 10
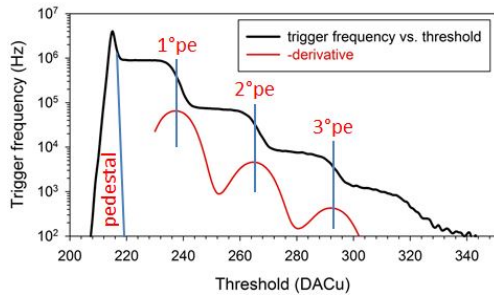
Fig. 9. The black profile is the staircase (integral distribution of the trigger frequency) of a single SiPM pixel. Pedestal represents the '0' photoelectron. The relative maxima of the negative derivative of the staircase (red curve) identify the 1st, 2nd and 3rd pe. The average distance between the 1st, the 2nd and the 3rd pe measures the pixel gain in DAC units.

shows the shaper output response of a pixel of the sensL arrayC 30035 SiPM to a luminous signal generated by a LED pulsed at 1 MHz.
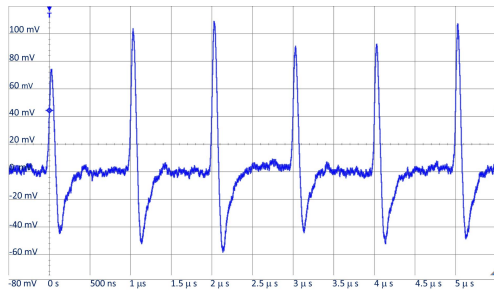
Fig. 10. Signal pulse height response demonstrating the correct behaviour of the shaper circuit.

5.5. Photon counting

Fig. 11 shows the set-up used to check photon counting performance. The pulse generator output, set to a 1.6 V amplitude with rising time of 690 ps and a falling time of 8 ns, gives rise to a 100 MHz sawtooth signal. Photon counting has been measured by injecting the pulse generator signal through a 60 db attenuator and a 100 pF capacitor generating

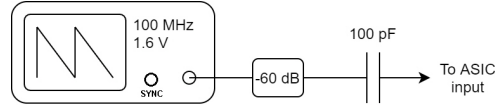a 160 fC signal at the ASIC input channel equivalent to a photoelectron every 10 ns.

Fig. 11. Photon counting set-up.

The RADIOROC differential trigger output is fed to the FPGA input and the trigger output is measured at the single-ended FPGA output. Fig. 12 shows the resulting trigger and the injected signal as recorded by the oscilloscope. It is evident that photon counting of 100 MHz is achieved and further trigger rate measurements indicate that trigger rate greater than 100 MHz is feasible.

5.6. Timing resolution

For timing applications, the dominant limitation on timing resolution with photodetectors is the fluctuation in the transit times of the electrons as they cascade through the detector. This causes a jitter in the arrival time of the pulse at the detector output. Timing resolution has been measured using the same experimental set-up shown in Fig. 11 but with an output frequency of 1 MHz and the sync output of the pulse generator used to trigger the oscilloscope (Lecroy WaveRunner 610Zi). RADIOROC jitter channel has been measured for various pre-amplifier gains and threshold values, taking into account the measured pulse generator jitter (18.4 ps). Fig. 13 shows the measured RMS jitter as a function of DAC unit for pre-amplifier gains of about 60 and 32 respectively and input signal equivalent to a photo-electron. RMS jitter is below 60 ps for both the pre-amplifier gains considered.

Fig. 14 shows a further Jitter measurement keeping a fixed threshold as injected charge value increases for the pre-amplifier gain, equal to 32 and 60 respectively.
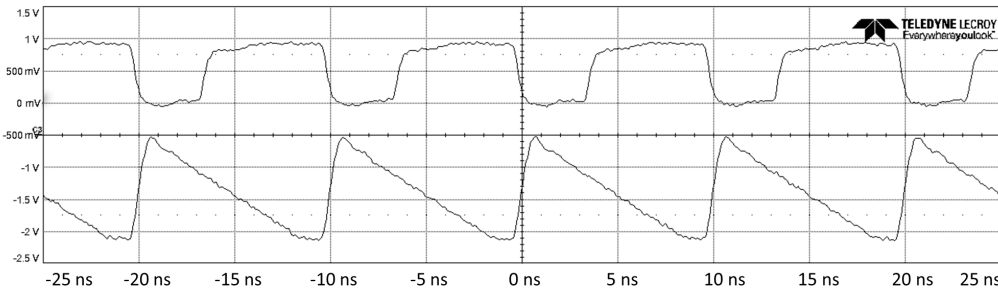
Fig. 12. Trigger output (top) and injected signal (bottom) at 100 *MHz*. The trigger signal is active low.
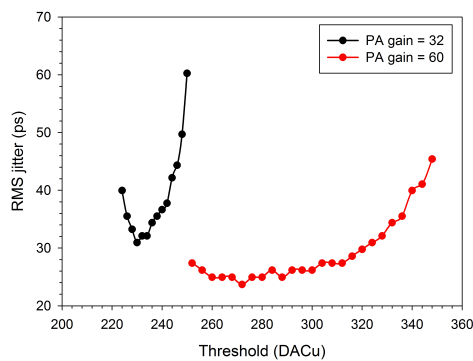

Fig. 13. RMS jitter for pre-amplifier gain=32 (black) and gain=60 (red) and for threshold values corresponding to 1 photo-electron.
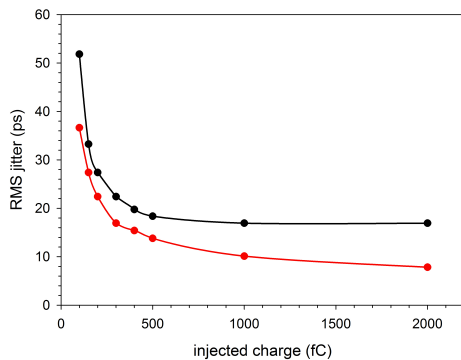

Fig. 14. RMS jitter with pre-amplifier gain=32 (black) and pre-amplifier gain=60 (red) as charge increases from 100 to 2000 *fC*.

6. Conclusions

The measurement of fluorescence and Cherenkov light as well as atmospheric phenomena, in case of space missions and of ground experiments, requires the detection of very faint and very intense light, with different time scale. Consequently, single photon counting and charge integration must coexist in the same FEE to achieve optimal performance. RADIOROC chip demonstrated to fulfill these requirements. Measurements have shown that the ASIC DC levels are compliant with the chip simulation. Input DAC and threshold DAC exhibit a linearity better than 0.1%. It has been demonstrated that RADIOROC achieves a photon counting rate up to 100 *MHz* (200 *MHz* is hopefully achievable) with a time resolution of less than 60 *ps* with an injected charge equivalent to one photo-electron. Although the measurements carried out have been successful, they do not represent the final results that foresee further improvements both in terms of the fine-tuning of all the available ASIC parameters and the improvement of the design in some of its parts.

Affiliations

5 Università degli Studi di Torino - Dipartimento di Fisica, Via Pietro Giuria 1, 10125 Torino, Italy

6 RIKEN, 2-1 Hirosawa, Wako, Saitama 351-0198, Japan

7 Istituto Nazionale di Fisica Nucleare - Sezione di Roma Tor Vergata, Via della Ricerca Scientifica, 00133 Roma, Italy

[8] Weeroc, 4 Avenue de la Baltique, 91140 Villebon sur Yvette, France

References

Acharya, B. S. et al. 2017, *Science with the Cherenkov Telescope Array*, arXiv:1709.07997

Antonelli, L. A., for the ASTRI Project 2021, *The ASTRI Mini-Array at Teide Observatory*, Proc. ICRC 2021, PoS(ICRC2021)897

Catalano, O., et al. 2016, *Volcanoes muon imaging using Cherenkov telescopes*, NIM/A, 807, 5-12

Catalano, O. 2018, *Cherenkov light for gamma astronomy and not only*, Mem. S.A.It., Vol. 89, 492

Contino, G., et al. 2020, *An ASIC front-end for fluorescence and Cherenkov light detection with SiPM for space and ground applications*, NIM/A, 980, 164510

Dova, M. T. et al. 2003, *The Pierre Auger Observatory*, Nuclear Physics B-Proceedings Supplements, 122, 170-178

Keilhauer, B., et al. 2013, *Nitrogen fluorescence in air for observing extensive air showers*, EPJ Web of Conferences, Vol. 53, 01010

Lombardi, S., et al. 2020, *First detection of the Crab Nebula at TeV energies with a Cherenkov telescope in a dual-mirror Schwarzschild-Couder configuration: the ASTRI-Horn telescope*, A&A, 634, A22

Olinto, A. V., et al. 2017, *POEMMA: probe of extreme multi-messenger astrophysics*, arXiv preprint arXiv:1708.07599

Pareschi, G., et al. 2013, *The dual-mirror Small Size Telescope for the Cherenkov Telescope Array*, Proc. 33rd ICRC

Takahashi, Y., et al. 2009, *The jem-euso mission*, New Journal of Physics, 11.6, 065009

Watson, A. A. 2011, *The discovery of Cherenkov radiation and its use in the detection of extensive air showers*, Nuclear Physics B-Proceedings Supplements, 212, 13-19